AIP | Journal of Applied Physics

# High-pressure study of the structural and elastic properties of defect-chalcopyrite HgGa2Se4

O. Gomis, R. Vilaplana, F. J. Manjón, D. Santamaría-Pérez, D. Errandonea et al.

Citation: J. Appl. Phys. **113**, 073510 (2013); doi: 10.1063/1.4792495
View online: http://dx.doi.org/10.1063/1.4792495
View Table of Contents: http://jap.aip.org/resource/1/JAPIAU/v113/i7
Published by the American Institute of Physics.

## Related Articles

High pressure phase transition of ZnO/SiO2 core/shell nanospheres
J. Appl. Phys. 113, 054314 (2013)

High pressure and high temperature stabilization of cubic AlN in Ti0.60Al0.40N
J. Appl. Phys. 113, 053515 (2013)

CO2-helium and CO2-neon mixtures at high pressures
J. Chem. Phys. 138, 044505 (2013)

High compressibility of rare earth-based bulk metallic glasses
Appl. Phys. Lett. 102, 031903 (2013)

Pressure-induced series of phase transitions in sodium azide
J. Appl. Phys. 113, 033511 (2013)

## Additional information on J. Appl. Phys.

Journal Homepage: http://jap.aip.org/
Journal Information: http://jap.aip.org/about/about_the_journal
Top downloads: http://jap.aip.org/features/most_downloaded
Information for Authors: http://jap.aip.org/authors

ADVERTISEMENT

AIP Advances
Now Indexed in Thomson Reuters Databases
Explore AIP's open access journal:
- Rapid publication
- Article-level metrics
- Post-publication rating and commenting

JOURNAL OF APPLIED PHYSICS **113**, 073510 (2013)

# High-pressure study of the structural and elastic properties of defect-chalcopyrite $HgGa_2Se_4$

O. Gomis,[1,a)] R. Vilaplana,[1] F. J. Manjón,[2] D. Santamaría-Pérez,[3] D. Errandonea,[4] E. Pérez-González,[5] J. López-Solano,[5] P. Rodríguez-Hernández,[5] A. Muñoz,[5] I. M. Tiginyanu,[6] and V. V. Ursaki[6]

[1]*Centro de Tecnologías Físicas: Acústica, Materiales y Astrofísica, MALTA Consolider Team, Universitat Politècnica de València, 46022 València, Spain*
[2]*Instituto de Diseño para la Fabricación y Producción Automatizada, MALTA Consolider Team, Universitat Politècnica de València, 46022 València, Spain*
[3]*Departamento de Química Física I, Universidad Complutense de Madrid, MALTA Consolider Team, Avenida Complutense s/n, 28040 Madrid, Spain*
[4]*Departamento de Física Aplicada-ICMUV, MALTA Consolider Team, Universidad de Valencia, Edificio de Investigación, C/Dr. Moliner 50, Burjassot, 46100 Valencia, Spain*
[5]*Departamento de Física Fundamental II, Instituto de Materiales y Nanotecnología, MALTA Consolider Team, Universidad de La Laguna, 38205 Tenerife, Spain*
[6]*Institute of Applied Physics, Academy of Sciences of Moldova, 2028 Chisinau, Moldova*

(Received 18 December 2012; accepted 1 February 2013; published online 20 February 2013)

In this work, we focus on the study of the structural and elastic properties of mercury digallium selenide ($HgGa_2Se_4$) which belongs to the family of $AB_2X_4$ ordered-vacancy compounds with tetragonal defect chalcopyrite structure. We have carried out high-pressure x-ray diffraction measurements up to 13.2 GPa. Our measurements have been complemented and compared with total-energy *ab initio* calculations. The equation of state and the axial compressibilities for the low-pressure phase of $HgGa_2Se_4$ have been experimentally and theoretically determined and compared to other related ordered-vacancy compounds. The theoretical cation-anion and vacancy-anion distances in $HgGa_2Se_4$ have been determined. The internal distance compressibility in $HgGa_2Se_4$ has been compared with those that occur in binary HgSe and $\varepsilon-$GaSe compounds. It has been found that the Hg-Se and Ga-Se bonds behave in a similar way in the three compounds. It has also been found that bulk compressibility of the compounds decreases following the sequence "$\varepsilon$-GaSe > $HgGa_2Se_4$ > HgSe." Finally, we have studied the pressure dependence of the theoretical elastic constants and elastic moduli of $HgGa_2Se_4$. Our calculations report that the low-pressure phase of $HgGa_2Se_4$ becomes mechanically unstable above 13.3 GPa. © *2013 American Institute of Physics*. [http://dx.doi.org/10.1063/1.4792495]

## I. INTRODUCTION

Mercury digallium selenide ($HgGa_2Se_4$) is one of the less studied adamantine-type $A^{II}B_2^{III}X_4^{VI}$ ordered-vacancy compounds (OVCs) which crystallizes in the tetragonal defect-chalcopyrite (DC) structure with space group (S.G.) I-4, Z = 2. OVCs are tetrahedrally coordinated semiconductors, which are derived from the diamond and the zincblende or sphalerite (F-43 m) structures. They have a vacant cationic site in an ordered and stoichiometric fashion, i.e., a stoichiometric vacancy is located at a fixed Wyckoff position in the unit cell.[1] The presence of vacancies in OVCs results in a complex physics for these compounds.

OVCs are important materials to understand the role played by vacancies in the physical and chemical properties of solids because they constitute a bridge between perfect and defect materials. Besides, they are interesting materials to study order-disorder phase transitions occurring in tetrahedral semiconductors. A common trend in all adamantine OVCs is that they have several non-equivalent tetrahedrally coordinated cations resulting in a distortion of the crystal lattice from the cubic symmetry. The lack of cubic symmetry provides special properties to OVCs with important applications in optoelectronics, solar cells, and non-linear optics.[1–4] These semiconductors are of interest as infrared-transmitting window materials among other applications. They are also applied in nonlinear optical devices and in narrow-band optical filters. In addition, OVCs are promising optoelectronic materials due to their high values of nonlinear susceptibility, optical activity, intense luminescence, and high photosensitivity.[2] They are interesting also in photovoltaics,[5] in diluted magnetic semiconductors,[6] and have already found practical applications as tunable filters and ultraviolet photodetectors.[7,8]

High-pressure (HP) studies on $A^{II}B_2^{III}X_4^{VI}$ compounds are receiving increasing attention in the last years.[9–26] In particular, the $AGa_2Se_4$ (A = Mn, Zn, and Cd) family has been studied by X-ray diffraction (XRD), Raman spectroscopy, and optical absorption. However, only few works have been devoted to the study of $HgGa_2Se_4$ under pressure. Recently, we reported optical absorption studies of DC-$CdGa_2Se_4$ and DC-$HgGa_2Se_4$ under pressure and focused on the explanation of the strong non-linear pressure dependence of their

a)Corresponding author, email: osgohi@fis.upv.es.

 © 2013 American Institute of Physics

direct band-gap energy.[25] A comprehensive work on DC-$CdGa_2Se_4$, where the pressure-induced order-disorder processes were discussed in detail, has been already published.[26]

In order to improve the knowledge of the HP behaviour of $AGa_2Se_4$ compounds, we report here HP-XRD measurements up to 13.2 GPa and *ab initio* total-energy calculations in DC-$HgGa_2Se_4$ to study in detail the structural and elastic properties of the low-pressure phase of $HgGa_2Se_4$. In particular, we have determined the equation of state (EOS) and the axial compressibilities of the low-pressure phase of $HgGa_2Se_4$. We have also carried out calculations of the elastic properties of DC-$HgGa_2Se_4$ and have studied its mechanical stability under pressure. The technical aspects of the experiments and calculations are described in Sects. II and III. The results are presented and discussed in Sec. IV. Finally, we present the conclusions of this work in Sec. V.

## II. EXPERIMENTAL SECTION

Single crystals of DC-$HgGa_2Se_4$ have been grown from its constituents HgSe and $Ga_2Se_3$ by chemical vapor transport method using iodine as a transport agent.[27] The as-grown crystals represent triangular prisms with mirror surfaces. Chemical and structural analyses have shown the stoichiometric composition of the crystals and no spurious phases have been observed. Ambient pressure x-ray diffraction and Raman spectroscopy confirmed that our sample has a DC-type structure.

We carried out HP angle-dispersive powder XRD experiments at room temperature. They were performed up to 13.2 GPa with an Oxford Xcalibur diffractometer using the Mo $K_\alpha$ radiation ($\lambda = 0.7107$ Å). Pressure was limited to 13.2 GPa to avoid the influence of deviatoric stresses and of precursor effects[28] associated with the phase transition observed in related compounds between 15 and 20 GPa.[14,20,22,23] The X-ray beam was collimated to a diameter of 300 $\mu$m. The same setup has been recently used to successfully characterize the high-pressure phases of sulfides and oxides.[29,30] XRD patterns were obtained on a 135 mm Atlas CCD detector placed at 110 mm from the sample. The samples were loaded in a modified Merrill-Basset diamond-anvil cell (DAC) with an angular aperture of $2\theta = 25°$. The diamond culets have a 500 $\mu$m diameter. $HgGa_2Se_4$ powder was loaded in the 150 $\mu$m-diameter hole of a stainless-steel gasket pre-indented to a thickness of 50 $\mu$m. A 4:1 methanol-ethanol mixture was used as quasi-hydrostatic pressure-transmitting medium (PTM).[31,32] Pressure was determined by the ruby fluorescence method.[33] Exposure times were typically of 1 h. The observed intensities were integrated as a function of $2\theta$ in order to give one-dimensional diffraction profiles. The indexing and refinement of the powder patterns were performed using CHECKCELL and POWDERCELL[34] program packages.

## III. THEORETICAL CALCULATION DETAILS

Total-energy calculations were performed within the framework of the density functional theory (DFT) and the pseudo-potential method using the Vienna *ab initio* simulation package (VASP).[35] The exchange and correlation energy has been taken in the generalized gradient approximation (GGA) according to the Perdew-Burke-Ernzerhof (PBE)[36] and the PBESol descriptions.[37] Details of total-energy calculations in the DC structure can be consulted in Ref. 25. *Ab initio* calculations allow the study of the mechanical properties of materials. The elastic constants describe the mechanical properties of a material in the region of small deformations, where the stress-strain relations are still linear. The elastic constants can be obtained by computing the macroscopic stress for a small strain with the use of the stress theorem.[38] Alternatively, the macroscopic stress can be also calculated using density functional perturbation theory (DFPT).[39] In the present work, we perform the evaluation of the elastic constants as implemented in the VASP code: the ground state and fully relaxed structures were strained in different directions according to their symmetry.[40] The total-energy variations were evaluated according to a Taylor expansion for the total energy with respect to the applied strain.[41] Due to this fact, it is important to check that the strain used in the calculations guarantees the harmonic behavior. This procedure allows us to obtain the $C_{ij}$ elastic constants in the Voigt notation where the number of independent elastic constants is reduced by crystalline symmetry.[42] We have used the generalized stability criteria in order to obtain information about the mechanical stability of the low-pressure phase of $HgGa_2Se_4$ from a theoretical point of view.

## IV. RESULTS AND DISCUSSION

### A. X-ray diffraction and structural properties

Table I shows the crystallographic parameters of our DC-$HgGa_2Se_4$ sample at 1 atm compared to our calculations and previous XRD experiments.[43,44] Our data agree with those of Refs. 43 and 44 and they are similar to our calculations. It must be stressed that GGA-PBE calculations tend to overestimate the lattice parameters while GGA-PBEsol calculations give results closer to those obtained experimentally.

In order to analyze the HP results, only the powder pattern below $2\theta = 18.3°$ is considered in the refinement process because of the appearance of the gasket peaks at higher angles. In this angular region the low-pressure phase has seven Bragg peaks which allow obtaining the pressure evolution of the unit-cell parameters. At the bottom of Fig. 1 we show in solid line the measured x-ray diffraction pattern of our sample at 0.4 GPa along with the Miller indexes of the Bragg reflections for the DC phase. Vertical marks representing the positions of the Bragg reflections are also plotted. Diffractograms up to 13.2 GPa could be indexed with the low-pressure DC phase. The diffraction peaks only move to higher angles as pressure increases, thus indicating that compression only cause a decrease of interplanar distances. It is observed the broadening of the diffraction peaks caused by the deterioration of the quasi-hydrostatic conditions of the experiment beyond 9 GPa.[31,45] Effects of deviatoric stresses on structural properties[46–48] apparently are not relevant in the pressure range covered by our experiments. However, a systematic study of the influence of deviatoric stress deserves a future systematic study.

TABLE I. Experimental and theoretical crystallographic parameters of tetragonal (I-4, Z = 2) $HgGa_2Se_4$ at room conditions. Hg, Ga(1), and Ga(2) are located at the 2 *a* (0,0,0), 2 *b* (0,0,0.5), and 2 *c* (0,0.5,0.25) Wyckoff positions, respectively. The vacancy is located at the 2 *d* (0,0.5,0.75) Wyckoff position. The relative atomic coordinates of the Se anion located at the 8 *g* (*x*,*y*,*z*) Wyckoff position are given in the table.

| | X-ray diffraction[a] | *Ab initio* PBE[b] | *Ab initio* PBEsol[b] | X-ray diffraction[c] | X-ray diffraction[d] |
|---|---|---|---|---|---|
| *a* (Å) | 5.711(1) | 5.860 | 5.736 | 5.715 | 5.693(1) |
| *c* (Å) | 10.814(1) | 10.985 | 10.810 | 10.78 | 10.826(4) |
| | *x* = 0.270(2) | x = 0.2754 | x = 0.2797 | x = 0.25 | x = 0.273(1) |
| | *y* = 0.245(5) | y = 0.2624 | y = 0.2563 | y = 0.25 | y = 0.2582(8) |
| Se site: 8 *g* | *z* = 0.1315(6) | z = 0.1393 | z = 0.1411 | z = 0.125 | z = 0.1382(6) |

[a]Our XRD measurements.
[b]Our calculations.
[c]Ref. 43.
[d]Ref. 44.

Figure 2 shows the pressure dependence of the lattice parameters for DC-$HgGa_2Se_4$ obtained from XRD experiments (solid circles) and from *ab initio* calculations. Experimental axial compressibilities for *a* and *c* axes at zero pressure, defined as $\kappa_x = \frac{-1}{x}\frac{\partial x}{\partial P}$ and obtained by fitting of a Murnaghan EOS,[49] are $\kappa_a = 9.2(6)\cdot10^{-3}$ GPa$^{-1}$ and $\kappa_c = 7.1(7)\cdot10^{-3}$ GPa$^{-1}$. These values show a compressibility anisotropy, being *a* the most compressible axis. This result agrees with previous results for other $AB_2X_4$ OVCs compounds.[14,20,22,23] Our theoretical results for the PBESol (PBE) description $\kappa_a = 10.2\cdot10^{-3}$ ($11.1\cdot10^{-3}$) GPa$^{-1}$ and $\kappa_c = 6.7\cdot10^{-3}$ ($9.6\cdot10^{-3}$) GPa$^{-1}$ agree reasonably well with the XRD experiment.

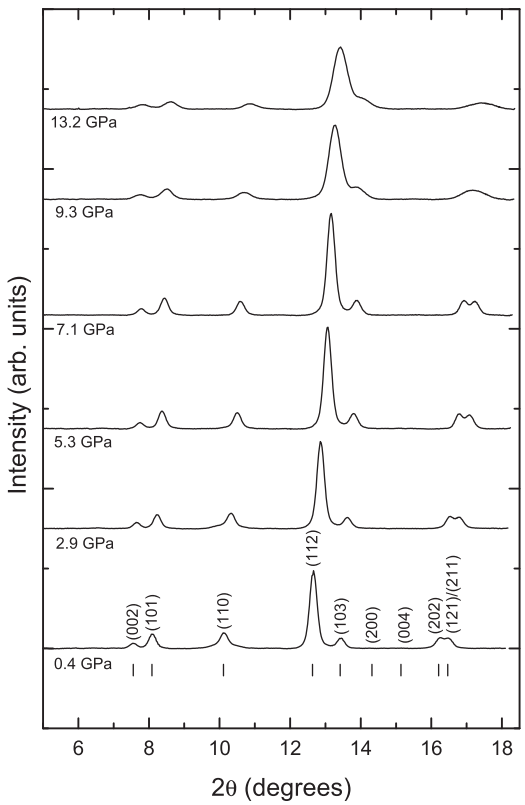


FIG. 1. Room temperature XRD patterns of $HgGa_2Se_4$ at selected pressures. In all diagrams, the background was subtracted. At 0.4 GPa, Bragg reflections are indicated with vertical ticks. Note that the (200) and (004) reflections are not seen because of their very low intensity which is less than 0.2% of the (112) peak intensity at 1 atm.

Figure 3 shows the volume of the DC phase vs. pressure. We have fitted these data with a third order Birch-Murnaghan (BM) EOS. All the experimental and theoretical values for the volume at zero pressure $V_0$, bulk modulus $B_0$, and its first-pressure derivative $B_0'$ are summarized in Table II. PBESol results are again in relatively good agreement with the experiment. Note that PBE yield a value for $B_0$ considerably lower than that obtained from the experiment, due to the large overestimation of the volume. Finally, we must stress that the obtained value for $B_0$ in DC-$HgGa_2Se_4$ from our experiment is very similar but slightly smaller than that obtained for DC-$CdGa_2Se_4$ ($B_0 = 41.5(2)$ GPa),[14] DC-$MnGa_2Se_4$ ($B_0 = 44(2)$ GPa),[20] DC-$CdAl_2Se_4$ ($B_0 = 52.1$ GPa),[21] and DS-$ZnGa_2Se_4$ ($B_0 = 47(2)$ GPa).[22]

Now we will analyze the pressure evolution of the *c*/*a* ratio in DC-$HgGa_2Se_4$ since the tetragonal distortion, $\delta = 2 - c/a$, could give important information. The inset of Fig. 3 shows the pressure dependence of the *c*/*a* vs. pressure. It can be observed that *c*/*a* increases with pressure from 1.89 at ambient pressure to 1.95 at 13.2 GPa. A similar experimental pressure dependence of the *c*/*a* ratio has been found in

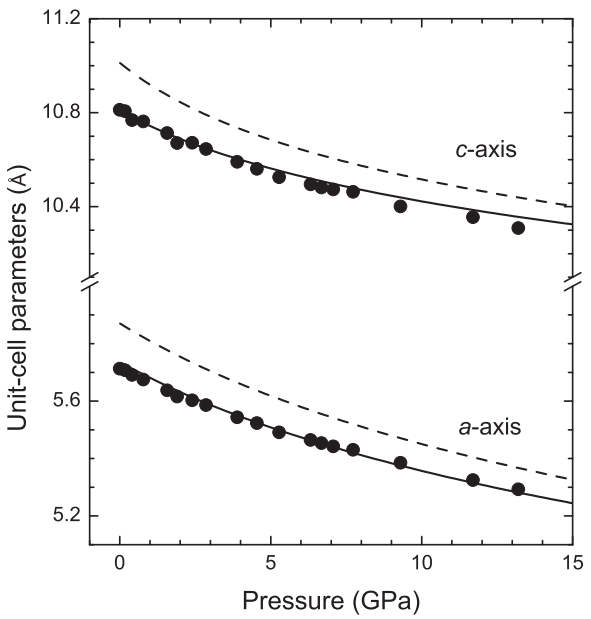


FIG. 2. Lattice parameters of the DC phase of $HgGa_2Se_4$ as a function of pressure. Solid circles refer to experimental data. *Ab initio* results are plotted with solid (PBESol) and dashed (PBE) lines.

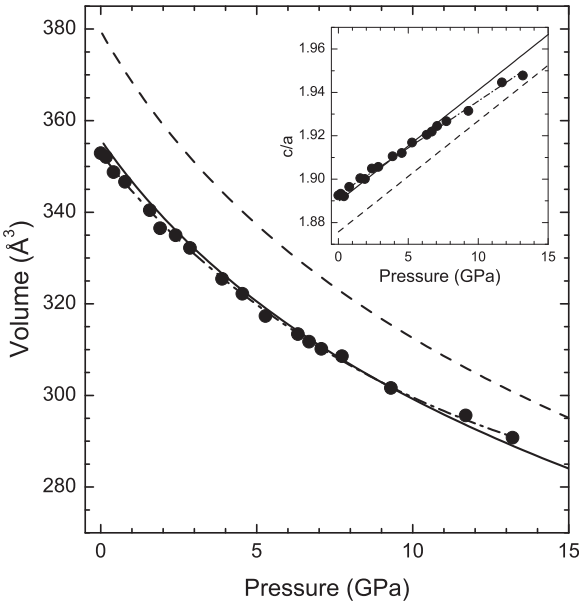


FIG. 3. Volume of the DC phase of $HgGa_2Se_4$ as a function of pressure. Experimental data (solid circles) and their EOS fit (dash-dotted line). Theoretical results are plotted with solid (PBESol) and dashed (PBE) lines. The inset shows the evolution of the *c*/*a* ratio of the DC phase as a function of pressure. Dash-dotted line is a linear fit to the experimental *c*/*a*.

DC-$CdGa_2Se_4$ and DC-$MnGa_2Se_4$.[14,20,26] It is noteworthy that $AGa_2X_4$ compounds ($A$ = Mn, Zn, Cd, Hg; $X$ = S, Se) with tetragonal DC structure at ambient pressure have *c*/*a* values close to 1.90,[14,20,50] while those with tetragonal defect stannite (DS) structure like $ZnGa_2Se_4$ or $ZnGa_2S_4$ have *c*/*a* ratios close to 1.98 at ambient pressure.[22,51] In the DS structure (S.G.: I-42 m, Z = 2), one Ga occupies the 2*a* Wyckoff position, the vacancy occupies the 2*b* Wyckoff site, and the other Ga and the Hg occupy the same 4*d* site with a site occupancy factor of 0.5 each one. In this way, the DS structure has cation disorder in the planes occupied with Hg and Ga atoms. This disorder has been used as an argument to propose that a *c*/*a* ratio close to 2 (i.e., a small tetragonal distortion) is an indication of a large cation-vacancy disorder in the structure.[44,50] This hypothesis is not supported by our results. They show that DC-$HgGa_2Se_4$, like other DC compounds,[14,20,26] tends to a more symmetric structure on compression. However, the increase of *c*/*a* on compression deduced from XRD experiments is well reproduced by calculations. Therefore, since there is no cation-vacancy disorder involved in our calculations, we conclude that the tetragonal distortion cannot be correlated with cation-vacancy disorder in the tetragonal structure at any pressure.[11]

According to Ref. 20, information on the cation-vacancy disorder could be obtained from the study of the pressure dependence of $\kappa_a$ and $\kappa_c$ and their difference. These dependences are shown for DC-$HgGa_2Se_4$ in the top, middle, and low panels of Fig. 4 for our XRD experiment, PBE, and PBESol calculations, respectively. As can be seen, in all cases the $\kappa_a$ and $\kappa_c$ compressibilities decrease with pressure as expected. The $\kappa_a$ - $\kappa_c$ difference is positive at every pressure but has a non-linear dependence with a positive pressure coefficient at low pressures and a negative pressure coefficient at high pressures, being the maximum value of $\kappa_a$ - $\kappa_c$ in the range 1.5-4 GPa. A similar evolution was found previously for DC-$MnGa_2Se_4$.[20] In that work, it was proposed that the change in tendency of $\kappa_a$ - $\kappa_c$ with pressure was a sign of the onset of the transformation from the DC to the DS phase. This would imply that cation-vacancy disorder is increasing with pressure above that pressure. However, our calculations show a maximum for $\kappa_a$ - $\kappa_c$ at a similar pressure than experiments despite cation-vacancy disorder is not considered in them. Therefore, we must conclude again that the change of the pressure coefficient of $\kappa_a$ - $\kappa_c$ cannot be taken as a measure of the cation-vacancy disorder in DC compounds.

In order to understand better the compression of the structure of DC-$HgGa_2Se_4$, we show in Figure 5(a) the evolution with pressure of the cation-anion and vacancy-anion distances of DC-$HgGa_2Se_4$ obtained from calculations. The largest distance is that of Hg-Se, the intermediate distances are those of Ga(1)-Se and Ga(2)-Se, and the shortest distance is that of vacancy-Se. Ga(1)-Se, Ga(2)-Se, and Hg-Se distances are much less compressible than the vacancy-Se, despite the vacancy-selenium distance is the smaller one. The high compressibility of the vacancy-Se distance is due to the weak repulsion between the separated electron distributions

TABLE II. Experimental and theoretical (Th.) volume ($V_0$), bulk modulus ($B_0$), and its pressure derivative ($B_0'$) here obtained for DC-$HgGa_2Se_4$ at zero pressure using a third-order BM EOS.

| | $V_0$ (Å$^3$) | $B_0$ (GPa) | $B_0'$ |
|---|---|---|---|
| Experimental | 352.9(6) | 39(2) | 5.2(4) |
| Th.(GGA-PBE) | 379.5(1) | 31.5(2) | 5.1(1) |
| Th.(GGA-PBESol) | 355.8(1) | 36.0(1) | 5.5(1) |

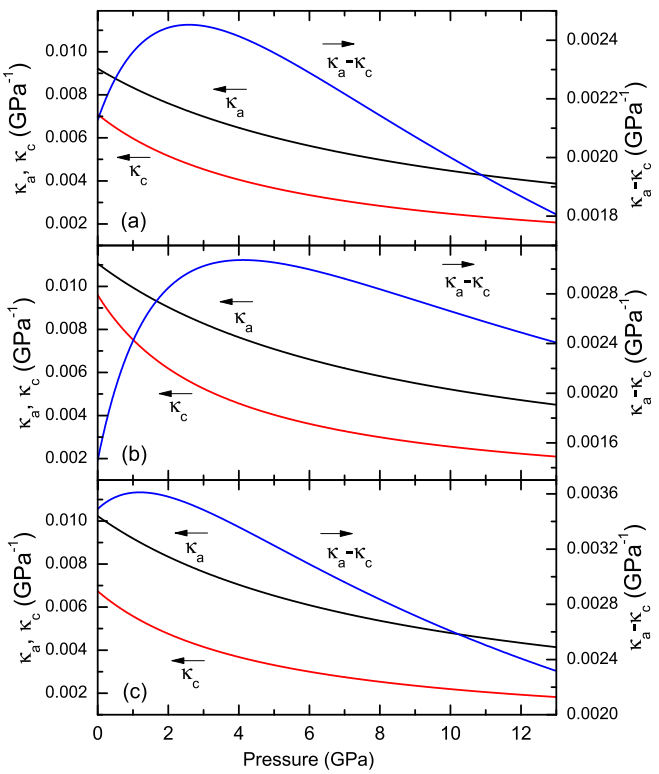


FIG. 4. Left side of panel: $\kappa_a$ and $\kappa_c$ vs. pressure. Right side: ($\kappa_a$ - $\kappa_c$) vs. pressure. Results correspond to: (a) XRD experiments, (b) PBE calculations, and (c) PBESol calculations.

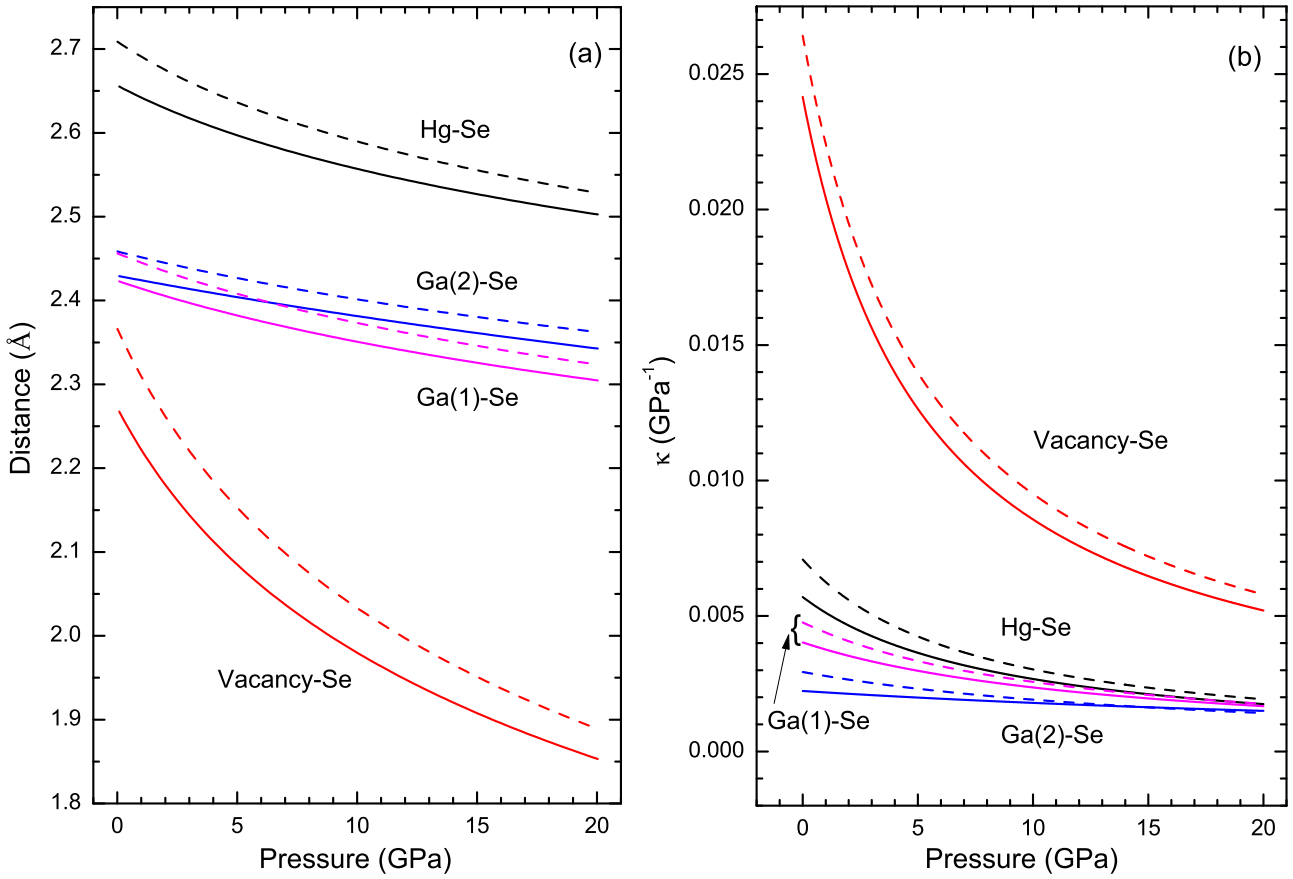


FIG. 5. Calculated cation-anion and vacancy-anion distances (a) and compressibilities (b) as a function of pressure for DC-$HgGa_2Se_4$. Solid (PBESol) and dashed (PBE) lines are used.

of Se atoms surrounding the vacancy. Consequently, Se atoms move towards the vacancy site at a faster rate than to the sites occupied by cations. These results for DC-$HgGa_2Se_4$ agree nicely with those obtained for DC-$CdGa_2Se_4$ from XRD measurements reported in Ref. 14.

A different perspective of the pressure dependence of the cation-anion and vacancy-anion internal distances for DC-$HgGa_2Se_4$ can be obtained by plotting the compressibility of those distances as a function of pressure [see Fig. 5(b)]. The distance compressibility decreases following the sequence "vacancy-Se > Hg-Se > Ga(1)-Se > Ga(2)-Se." At HP, the cation-anion distance compressibility tends to approach to a similar value whilst the vacancy-Se distance compressibility is still the most compressible one. The calculated compressibility at zero pressure for the Hg-Se, average Ga(1)-Se and Ga(2)-Se, and vacancy-Se distances is summarized in Table III.

Finally, we have carried out a comparative study of the compressibility of the Hg-Se and the average Ga-Se bonds in DC-$HgGa_2Se_4$ with those of the Hg-Se and Ga-Se bonds in the binary compounds HgSe and ε-GaSe. Results are summarized in Table III. HgSe has a cubic unit cell with a zinc-blende structure (S.G.: F-43m, Z = 4),[52] while ε-GaSe has a hexagonal unit cell with a laminar structure consisting of a four-sheet sequence of planes of Se-Ga-Ga-Se (S.G.: P-6m2, Z = 4).[53] For the case of HgSe we have calculated, the Hg-Se bond compressibility from *ab initio* results taken from Ref. 54 with both the PBE and the PBESol description, whereas for the case of ε-GaSe, we have calculated the Ga-Se bond compressibility from *ab initio* results taken from Ref. 55 with the GGA description. Curiously, the Hg-Se bond compressibility is similar in both DC-$HgGa_2Se_4$ and

TABLE III. Distance compressibility κ (in $10^{-3}$ $GPa^{-1}$) obtained from our calculations at zero pressure. For DC-$HgGa_2Se_4$, data of the Hg-Se, average Ga-Se, and vacancy-Se distances are shown. For HgSe, data of the Hg-Se distance are shown. For ε-GaSe, data of Ga-Se and Se(1)-Se(2) distances are shown. Theoretical (th.) and experimental (exp.) values for $B_0$ (in GPa) at zero pressure are also included.

| | $HgGa_2Se_4$ | HgSe | ε-GaSe |
|---|---|---|---|
| κ(Hg-Se) (th.) | 7.1[a], 5.7[b] | 7.7[c], 6.4[d] | |
| κ(Ga-Se) (th.) | 3.9[a], 3.1[b] | | 3.4[e] |
| κ(vacancy-Se) (th.) | 26.4[a], 24.2[b] | | |
| κ[Se(1)-Se(2)] (th.) | | | 35.8[e] |
| $B_0$ (th.) | 31.5(2)[a], 36.0(1)[b] | 42[f], 51[g] | 28.3[h] |
| $B_0$ (exp.) | 39(2)[i] | 49.7[j] | 34(2)[k], 34.4[l], 33.1[m] |

[a,b]Our calculations with GGA-PBE and GGA-PBESol description, respectively.
[c,d]Obtained with structural data taken from Ref. 54 with GGA-PBE and GGA-PBESol description, respectively.
[e]Obtained with structural data taken from Ref. 55.
[f,g]Ref. 54 with GGA-PBE and GGA-PBESol description, respectively.
[h]Ref. 56.
[i]Our XRD experiment.
[j]$B_0$ is obtained from the elastic constants given in Ref. 57.
[k]Ref. 55.
[l,m]$B_0$ is obtained using the Hill approximation[58] from the elastic constants measured in Refs. 59 and 60, respectively.

HgSe, and the Ga-Se bond compressibility is similar in both DC-$HgGa_2Se_4$ and ε-GaSe. It is also interesting to calculate the Se(1)-Se(2) bond compressibility in ε-GaSe (see Table III), where Se(1) and Se(2) are anions located in adjacent sheets linked together by van der Waals interactions. The compressibility of the Se(1)-Se(2) distance in ε-GaSe is the greatest one followed by the compressibility of the vacancy-Se distance in DC-$HgGa_2Se_4$. These results suggest that the bulk compressibility (modulus) in the three compounds under comparison should decrease (increase) following the sequence "ε-GaSe-DC-$HgGa_2Se_4$–HgSe." That is, following the sequence "laminar compound-OVC-zincblende-type compound without vacancies." This hypothesis is verified by the values of the bulk modulus at zero pressure obtained both theoretically and experimentally and summarized in Table III. This result indicates that the bulk compressibility at zero pressure of the laminar compound is mainly determined by the compressibility of the Se(1)-Se(2) distance due to the van der Waals interaction between Se atoms along the *c* axis and that the bulk compressibility of the OVCs is mainly determined by the compressibility of the vacancy-anion distance due to the presence of stoichiometric vacancies in the unit cell.

### B. Elastic properties

Compounds crystallizing in the DC phase belong to the tetragonal Laue group TII. This Laue group contains all crystals with 4, −4, and 4/*m* point groups. In this group, there are seven independent second-order elastic constants which are $C_{11}$, $C_{12}$, $C_{13}$, $C_{33}$, $C_{44}$, $C_{66}$, and $C_{16}$. On the other hand, in the tetragonal Laue group TI, which contains all crystals with 422, 4*mm*, −42*m*, and 4/*mmm* point groups, there are six independent second-order elastic constants which are: $C'_{11}$, $C'_{12}$, $C'_{13}$, $C'_{33}$, $C'_{44}$, and $C'_{66}$. The formulas for the calculation of the elastic moduli with the use of the elastic constants in the Laue group TII have not been derived analytically. This is due to the presence of the off-diagonal shear elastic constant $C_{16}$ which is not normally zero. However, it is possible to transform the seven components $C_{ij}$ of the elastic tensor of a TII crystal into the six components $C'_{ij}$ of the elastic tensor of a TI crystal. For that purpose one needs to make $C'_{16}$ equal to zero by means of a rotation around the *z* axis with the angle given by:[61]

$$\phi_{\kappa,\gamma} = \frac{1}{4}\arctan\left(\frac{4C_{16}}{C_{11} - C_{12} - 2C_{66}}\right). \quad (1)$$

Equation (1) gives two values for $\phi$ in the range $0 < \varphi < |\pi/2|$ that correspond to $\phi_\kappa$ and $\phi_\gamma$ where $\phi_\gamma = \phi_\kappa + \pi/4$.[61,62] For DC-$HgGa_2Se_4$ at zero pressure, we obtain $\phi_\kappa = 0.76°$ and $\phi_\gamma = 45.76°$. The small value for $\phi_k$ is because of the small value of $C_{16} = -0.3$ GPa obtained at zero pressure. The equations used to obtain the six independent $C'_{ij}$ elastic constants of a TI crystal as a function of the seven $C_{ij}$ elastic constants of a TII crystal and the $\phi$ angle are taken from Ref. 62.

We report in Table IV the set of seven elastic constants $C_{ij}$ at zero pressure obtained from our calculations with the PBESol description together with the two sets of six $C'_{ij}$ obtained for angles $\phi_\kappa$ and $\phi_\gamma$. The calculations have been carried out using the PBESol prescription as it is the one that better mimics the structural parameters for the crystal. In Table IV, it is also included theoretical results for the seven $C_{ij}$ elastic constants of DC-$CdGa_2Se_4$ and DC-$CdGa_2S_4$.[63] In general, the values for $C_{ij}$ are similar in both DC-$HgGa_2Se_4$ and DC-$CdGa_2Se_4$. We must note that with the $C_{ij}$ reported for DC-$CdGa_2S_4$, we obtain a value of the bulk modulus in the Reuss approximation[64] of 40.6 GPa instead of the value of 58.4 GPa reported by the authors. In this sense, we think that there could be a mistake in the reported values for the $C_{ij}$ of DC-$CdGa_2S_4$ since we expect that $B_0$ should be around 60 GPa in DC-$CdGa_2S_4$.

With the set of six elastic constants for DC-$HgGa_2Se_4$, standard formulas for the bulk (*B*) and shear (G) moduli of the tetragonal Laue group TI in the Voigt,[65] Reuss,[64] and Hill[58] approximations, labeled with subscripts *V*, *R*, and *H*, respectively, can be then applied:[66]

$$B_V = \frac{2C_{11} + C_{33} + 2C_{12} + 4C_{13}}{9}, \quad (2)$$

$$B_R = \frac{1}{2S_{11} + S_{33} + 2S_{12} + 4S_{13}}, \quad (3)$$

$$B_H = \frac{B_V + B_R}{2}, \quad (4)$$

TABLE IV. Seven $C_{ij}$ elastic constants (in GPa) for DC-$HgGa_2Se_4$. The set of six $C'_{ij}$ ($C'_{16} = 0$) elastic constants are also given. The elastic moduli *B*, *G*, and *E* (in GPa) and Possion's ratio (ν) are given in the Voigt, Reuss, and Hill approximations, labeled, respectively, with subscripts *V*, *R*, and *H*. The *B*/*G* ratio and the shear anisotropy factor (*A*) are also given. The values for $\kappa_a$ and $\kappa_c$ have been obtained from the $S_{ij}$ elastic compliances tensor by using Eqs. (10). All given data has been calculated with the PBESol prescription at zero pressure. Calculated data for DC-$CdGa_2Se_4$ and DC-$CdGa_2S_4$ are also added.[63]

| | DC-$HgGa_2Se_4$[a] | DC-$CdGa_2Se_4$[b] | DC-$CdGa_2S_4$[b] |
|---|---|---|---|
| $C_{11}$ | 54.2 | 52.5 | 61.8 |
| $C_{12}$ | 24.3 | 20.4 | 24.7 |
| $C_{13}$ | 31.2 | 38.8 | 35.7 |
| $C_{33}$ | 55.5 | 60.0 | 50.0 |
| $C_{44}$ | 29.9 | 31.6 | 33.9 |
| $C_{66}$ | 26.2 | 16.0 | 27.0 |
| $C_{16}$ | −0.3 | −1.9 | −2.7 |
| $C'_{11}$ | 54.2[c], 65.5[d] | | |
| $C'_{12}$ | 24.3[c], 13.0[d] | | |
| $C'_{13}$ | 31.2[c], 31.2[d] | | |
| $C'_{33}$ | 55.5[c], 55.5[d] | | |
| $C'_{44}$ | 29.9[c], 29.9[d] | | |
| $C'_{66}$ | 26.2[c], 14.9[d] | | |
| $B_V, B_R, B_H$ | 37.5, 37.2, 37.4 | 36.1 | 58.4[e] |
| $G_V, G_R, G_H$ | 22.3, 18.8, 20.6 | | |
| $E_V, E_R, E_H$ | 55.9, 48.4, 52.2 | | |
| $\nu_V, \nu_R, \nu_H$ | 0.25, 0.28, 0.27 | | |
| $B_V/G_V, B_R/G_R, B_H/G_H$ | 1.68, 1.98, 1.81 | | |
| *A* | 1.75[c], 0.57[d] | | |
| $\kappa_a, \kappa_c$ ($10^{-3}$ GPa$^{-1}$) | 10.1, 6.7 | | |

[a]Our calculations with GGA-PBESol prescription.
[b]Data taken from Ref. 63.
[c,d]Rotation angle of $\phi_\kappa = 0.76°$ and $\phi_\gamma = 45.76°$, respectively.
[e]We obtained for $B_R$ a value of 40.6 GPa from the $C_{ij}$ data given by Ref. 63.

$$G_V = \frac{2C_{11} + C_{33} - C_{12} - 2C_{13} + 6C_{44} + 3C_{66}}{15}, \quad (5)$$

$$G_R = \frac{15}{8S_{11} + 4S_{33} - 4S_{12} - 8S_{13} + 6S_{44} + 3S_{66}}, \quad (6)$$

$$G_H = \frac{G_V + G_R}{2}. \quad (7)$$

In the Reuss approximation, we use formulas for $B_R$ and $G_R$ obtained from the elastic compliance $S'_{ij}$ tensor (the inverse of the elastic constant $C'_{ij}$ tensor). In the Voigt (Reuss) approximation, uniform strain (stress) is assumed throughout the polycrystal.[64,65] On the other hand, Hill has shown that the Voigt and Reuss averages are limits and suggested that the actual effective $B$ and $G$ elastic moduli can be approximated by the arithmetic mean of the two bounds.[58] The Young ($E$) modulus and the Poisson's ratio ($\nu$) are calculated with the expressions:[66,67]

$$E_X = \frac{9B_X G_X}{G_X + 3B_X}, \quad (8)$$

$$\nu_X = \frac{1}{2}\left(\frac{3B_X - 2G_X}{3B_X + G_X}\right), \quad (9)$$

where the subscript $X$ refers to the symbols $V$, $R$, and $H$. In Table IV, we summarize all the values obtained of the $B$, $G$, and $E$ for DC-$HgGa_2Se_4$ at zero pressure in the Voigt, Reuss, and Hill approximations. Note that we have obtained a value for the bulk modulus in the Hill approximation of $B_H = 37.4$ GPa which is in very good agreement with the value of $B_0 = 36.0(1)$ GPa obtained from our PBESol structural calculations via a third-order BM EOS fit. This result gives us confidence about the correctness of our elastic constants calculations.

Table IV also includes the values of the ratio between the bulk and shear modulus, $B/G$, and the shear anisotropy factor $A$. The $B/G$ ratio has been proposed by Pugh to predict brittle or ductile behavior of materials.[68] According to the Pugh criterion, a $B/G$ value above 1.75 indicates a tendency for ductility; otherwise, the material behaves in a brittle manner. In our particular case, we found a value of B/G = 1.81 in the Hill approximation indicating that the material should be ductile but close to the limit of ductility at zero pressure. The shear anisotropy factor $A$ for our tetragonal cell is defined as $A = 2C_{66}/(C_{11}\text{-}C_{12})$.[69] If $A$ is equal to one, no anisotropy exists. On the other hand, the more this parameter differs from one, the more elastically anisotropic is the crystalline structure. In our particular case, $A = 1.75$ and 0.57 for angles $\phi_\kappa$ and $\phi_\gamma$, respectively. These values are rather different from 1 and evidence the anisotropy of our tetragonal cell at zero pressure. Note that the anisotropy factors obtained for the two possible rotation angles follow the relation $0.57 = 1/1.75$, which is a direct consequence of the $\pi/4$ rotation around the z axis ($\phi_\gamma = \phi_\kappa + \pi/4$). We have also obtained the axial compressibilities $\kappa_a$ and $\kappa_c$ from the elastic constants. The used formulas are:[62]

$$\kappa_a = S_{11} + S_{12} + S_{13} \quad \text{and} \quad \kappa_c = 2S_{13} + S_{33}, \quad (10)$$

where $S_{ij}$ refers to components of the elastic compliances tensor. Table IV includes the values for $\kappa_a$ and $\kappa_c$ obtained at zero pressure using Eq. (10) which are in very good agreement with those reported in Fig. 4(c). Again, this result gives us confidence about the correctness of our elastic constants calculations.

In the following, we are going to study the mechanical stability of DC-$HgGa_2Se_4$ at HP. A lattice is mechanically stable only if the elastic energy change associated with an arbitrary deformation given by small strains is positive for any small deformation.[70] This implies restrictions on the $C_{ij}$ elastic constants that are mathematically expressed by the fact that the principal minors of the determinant with elements $C_{ij}$ are all positive.[71] The latter restrictions are often called the Born-Huang stability criteria and for the case of a tetragonal crystal with six $C_{ij}$ elastic constants, the mechanical stability at zero pressure requires that:[70]

$$C_{11} > 0, \quad C_{44} > 0, \quad C_{66} > 0, \quad C_{11} - C_{12} > 0 \quad (11)$$

and

$$C_{11}C_{33} + C_{12}C_{33} - 2C_{13}^2 > 0. \quad (12)$$

In our particular case, all the above criteria are satisfied for DC-$HgGa_2Se_4$ at zero pressure and the tetragonal crystal is mechanically stable at zero pressure, as expected. In order to study the mechanical stability of the tetragonal phase at HP, one has to study the evolution of the elastic constants as pressure increases. Figure 6(a) shows the evolution of the

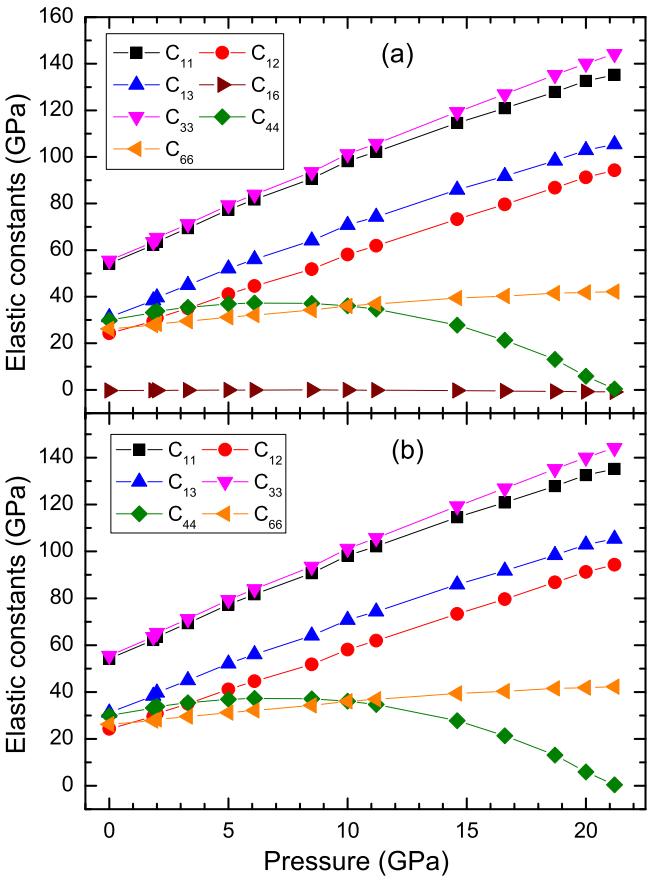


FIG. 6. Pressure dependence of the theoretical (PBESol) elastic constants of DC-$HgGa_2Se_4$: (a) Seven $C_{ij}$ elastic constants and (b) Six $C'_{ij}$ elastic constants. Solid lines connecting the calculated data points are shown as a guide to the eyes.

seven calculated $C_{ij}$ of DC-$HgGa_2Se_4$ with pressure. It can be seen that the $C_{11}$, $C_{12}$, $C_{13}$, $C_{33}$, and $C_{66}$ elastic constants increase monotonically as pressure increases. The $C_{44}$ elastic constant increases up to a value of 8 GPa and above that pressure decreases as pressure increases. In the case of the $C_{16}$ elastic constant, it increases up to a value of −0.05 GPa at about 7.5 GPa and then decreases reaching a value of −0.9 GPa at 21 GPa. In any case, $C_{16}$ remains small in all the studied pressure range.

In order to study the mechanical stability of the tetragonal phase under pressure Eqs. (11) and (12) have to be modified to include the particular case when the external load is different from zero. For a detailed explanation of how the Born stability criteria must be modified when the solid is subject to a external load, we refer the reader to Refs. 70 and 72–74. The general stability criteria valid when the tetragonal TI crystal is subjected to an external hydrostatic pressure $P$ take the form:[70,74]

$$C_{11} - P > 0, \tag{13}$$

$$C_{44} - P > 0, \tag{14}$$

$$C_{66} - P > 0, \tag{15}$$

$$C_{11} - C_{12} - 2P > 0, \tag{16}$$

$$(C_{33} - P)(C_{11} + C_{12}) - 2(C_{13} + P)^2 > 0. \tag{17}$$

We note that the general stability criteria shown with Eqs. (13) to (17) are applicable to a tetragonal crystal with six elastic constants. In this way, we plot in Figure 6(b), the evolution with pressure of the six elastic constants for the case of $\phi_\kappa = 0.76°$ and check whether DC-$HgGa_2Se_4$ satisfies Eqs. (13) to (17) for all pressures or not. It is found that Eq. (17) is violated at 13.3 GPa, Eq. (14) is violated at 17.5 GPa, and Eq. (16) is violated at 20.5 GPa. We highlight the fact that the pressures at which we find that the three equations are violated are the same for both $\phi_\kappa$ and $\phi_\gamma$ transformations. On the other hand, it is interesting to comment that Eq. (17), that in the particular case of $P = 0$ GPa reduces to Eq. (12), is the numerator of the expression for the bulk modulus in the Reuss approximation when $B_R$ is expressed as a function of $C_{ij}$ components.[74] Therefore, our study of the mechanical stability of DC-$HgGa_2Se_4$ at HP suggests that the tetragonal phase becomes mechanically unstable beyond 13.3 GPa. This pressure is consistent with the pressure at which dark linear defects appear in absorption experiments.[25]

To conclude we would like to comment on the pressure dependence of the elastic moduli ($B$, $G$ and $E$), the $\nu$ Poisson's ratio, the $B/G$ ratio, and the $A$ factor reported in Fig. 7. It is found that the bulk modulus increases as pressure increases reaching a value of $B_H = 83.6$ GPa at 13 GPa. The shear modulus increases with pressure reaching a maximum value of $G_H = 25.9$ GPa at 10.5 GPa and above that pressure

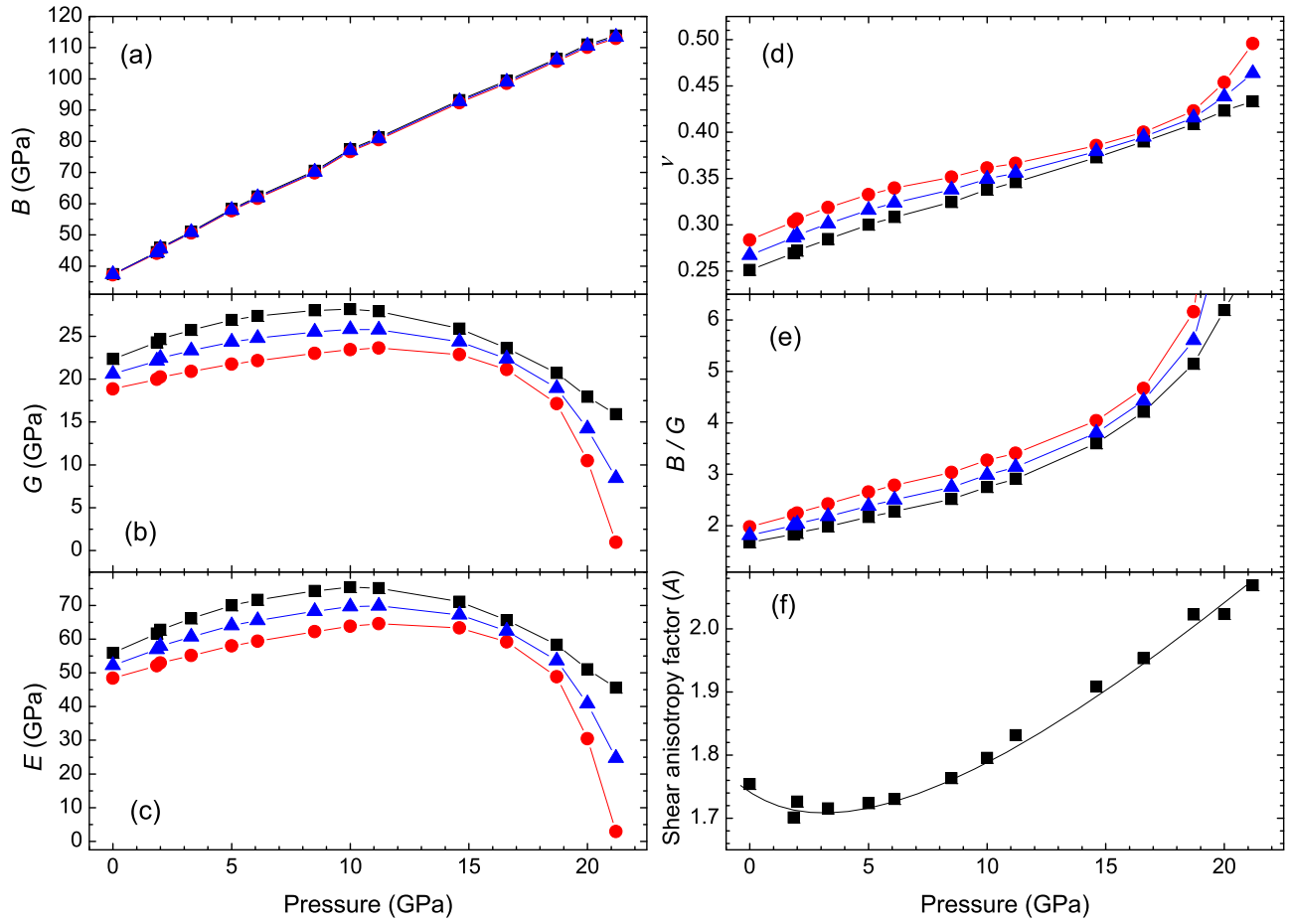


FIG. 7. Pressure dependence of (a) $B$, (b) $G$, (c) $E$, (d) $\nu$, (e) $B/G$, and (f) $A$. Squares, circles, and triangles refer to the Voigt, Reuss, and Hill approximations. $A$ factor data are shown for $\phi_\kappa = 0.76°$. Solid lines connecting the calculated data points are shown as a guide to the eyes in panels (a) to (e). Solid line in panel (f) represents the behavior of $A$ with pressure.

it decreases as pressure increases. In the case of the Young modulus, it increases with pressure reaching a maximum value of $E_H = 69.8$ GPa at 10.8 GPa and above that pressure it decreases as pressure increases. The Poisson's ratio and the $B/G$ ratio increase as pressure increases reaching a value $\nu_H = 0.37$ and $B_H/G_H = 3.50$ at 13 GPa. In the case of the shear anisotropy factor $A$, it is found that for $\phi_\kappa = 0.76°$, $A$ decreases slightly reaching a minimum value 1.71 at 3.0 GPa and above that pressure it increases with pressure reaching a value of 1.86 at 13 GPa. The change of the pressure coefficient of the theoretically calculated $G$ and $E$ elastic moduli at high pressures seems to be related to the mechanical instability of the DC structure above 13 GPa. These behaviors could be related to the onset of the cation-vacancy disorder process that occurs in DC-$HgGa_2Se_4$ above this pressure that it is evidenced by the appearing of dark linear defects in absorption measurements, as already commented. In this sense, more experimental and theoretical work is needed to confirm if the coincidence between the pressure for the appearance of dark linear defects and that of the mechanical instability happens in other DC compounds, and therefore, they can be considered as related phenomena.

## V. CONCLUSIONS

We have performed HP-XRD measurements in DC-$HgGa_2Se_4$ and have compared the experimental results with *ab initio* calculations. The axial compressibilities and the EOS of tetragonal DC-$HgGa_2Se_4$ have been obtained showing that DC-$HgGa_2Se_4$ behaves in a similar way to other $AGa_2Se_4$ ($A$ = Mn, Zn, Cd) adamantine OVCs and in particular to DC-$CdGa_2Se_4$.

A comparative study of the compressibility of the internal distances in DC-$HgGa_2Se_4$ and the compressibility of the Hg-Se and Ga-Se bonds in the binaries HgSe and ε-GaSe shows that the Hg-Se and Ga-Se bonds behave in a similar way in the three compounds. However, the bulk compressibility of the three compounds decreases following the sequence "ε-GaSe > DC-$HgGa_2Se_4$ > HgSe," i.e., the binary layered ε-GaSe compound, characterized by a van der Waals interaction between the layers, is more compressible than the defect chalcopyrite structure, which contains stoichiometric vacancies, and this structure is more compressible than zincblende-type HgSe that has no vacancies in its structure.

Finally, a detailed theoretical study of the elastic properties of DC-$HgGa_2Se_4$ has been accomplished. At zero pressure, the theoretical elastic constants and elastic moduli obtained for the tetragonal phase are in agreement with other calculations for similar compounds. Additionally, we have reported the HP evolution of the elastic constants and have performed a study of the mechanical stability of the tetragonal phase at HP. We have found that the low-pressure tetragonal phase of DC-$HgGa_2Se_4$ should become mechanically unstable at pressures above 13.3 GPa.

## ACKNOWLEDGMENTS

This study was supported by the Spanish government MEC under Grants No: MAT2010-21270-C04-01/03/04 and CTQ2009-14596-C02-01, by the Comunidad de Madrid and European Social Fund (S2009/PPQ-1551 4161893), by MALTA Consolider Ingenio 2010 project (CSD2007-00045), and by the Vicerrectorado de Investigación y Desarrollo of the Universidad Politécnica de Valencia (UPV2011-0914 PAID-05-11 and UPV2011-0966 PAID-06-11). E.P.-G., J.L.-S., A.M., and P.R.-H. acknowledge computing time provided by Red Española de Supercomputación (RES) and MALTA-Cluster.

[1]A. MacKinnon, in *Tables of Numerical Data and Functional Relationships in Science and Technology*, edited by O. Madelung, M. Schulz, and H. Weiss, Landolt-Börnstein New Series, Group III, Vol. 17, pt. h (Springer-Verlag, Berlin, 1985), p. 124.
[2]A. N. Georgobiani, S. I. Radautsan, and I. M. Tiginyanu, Sov. Phys. Semicond. **19**, 121 (1985).
[3]J. E. Bernard and A. Zunger, Phys. Rev. B **37**, 6835 (1988).
[4]X. Jiang and W. R. L. Lambrecht, Phys. Rev. B **69**, 035201 (2004).
[5]A. Zunger, S. Wagner, and P. M. Petroff, J. Electron. Mater. **22**, 3 (1993).
[6]A. Millan and M. C. Moron, J. Appl. Phys. **89**, 1687 (2001).
[7]S. I. Radautsan and I. M. Tiginyanu, Jpn. J. Appl. Phys. **32S3**, 5 (1993). Available at: http://jjap.jsap.jp/link?JJAPS/32S3/5.
[8]N. V. Joshi, J. Luengo, and F. Vera, Mater. Lett. **61**, 1926 (2007).
[9]I. I. Burlakov, Y. Raptis, V. V. Ursaki, E. Anastassakis, and I. M. Tiginyanu, Solid State Commun. **101**, 377 (1997).
[10]J. González, R. Rico, E. Calderón, M. Quintero, and M. Morocoima, Phys. Status. Solidi.B **211**, 45 (1999).
[11]V. V. Ursaki, I. I. Burlakov, I. M. Tiginyanu, Y. S. Raptis, E. Anastassakis, and A. Anedda, Phys. Rev. B **59**, 257 (1999).
[12]M. Fuentes-Cabrera and O. F. Sankey, J. Phys.: Condens. Matter **13**, 1669 (2001).
[13]M. Fuentes-Cabrera, J. Phys.: Condens. Matter **13**, 10117 (2001).
[14]A. Grzechnik, V. V. Ursaki, K. Syassen, I. Loa, I. M. Tiginyanu, and M. Handfland, J. Solid State Chem. **160**, 205 (2001).
[15]T. Mitani, S. Onari, K. Allakhverdiev, F. Gashimzade, and T. Kerimova, Phys. Status Solidi B **223**, 287 (2001).
[16]A. Tatsi, D. Lampakis, E. Liarokapis, S. A. López, L. Martínez, and W. Giriat, High Press. Res. **22**, 89 (2002).
[17]I. M. Tiginyanu, V. V. Ursaki, F. J. Manjón, and V. E. Tezlevan, J. Phys. Chem. Solids **64**, 1603 (2003).
[18]T. Mitani, T. Naitou, K. Matsuishi, S. Onari, K. Allakhverdiev, F. Gashimzade, and T. Kerimova, Phys. Status Solidi B **235**, 321 (2003).
[19]K. Allakhverdiev, F. Gashimzade, T. Kerimova, T. Mitani, T. Naitou, K. Matsuishi, and S. Onari, J. Phys. Chem. Solids **64**, 1597 (2003).
[20]J. Marquina, Ch. Power, P. Grima, M. Morocoima, M. Quintero, B. couzinet, J. C. Chervin, P. Munsch, and J. González, J. Appl. Phys. **100**, 093513 (2006).
[21]S. Meenakshi, V. Vijyakumar, B. K. Godwal, A. Eifler, I. Orgzall, S. Tkachev, and H. D. Hochheimer, J. Phys. Chem. Solids **67**, 1660 (2006).
[22]D. Errandonea, R. S. Kumar, F. J. Manjón, V. V. Ursaki, and I. M. Tiginyanu, J. Appl. Phys. **104**, 063524 (2008).
[23]S. Meenakshi, V. Vijyakumar, A. Eifler, and H. D. Hochheimer, J. Phys. Chem. Solids **71**, 832 (2010).
[24]P. Singh, M. Sharma, U. P. Verma, and P. Jensen, Z. Kristallogr. **225**, 508 (2010).
[25]F. J. Manjón, O. Gomis, P. Rodríguez-Hernández, E. Pérez-González, A. Muñoz, D. Errandonea, J. Ruiz-Fuertes, A. Segura, M. Fuentes-Cabrera, I. Tiginyanu, and V. V. Ursaki, Phys. Rev. B **81**, 195201 (2010).
[26]O. Gomis, R. Vilaplana, F. J. Manjón, E. Pérez-González, J. López-Solano, P. Rodríguez-Hernández, A. Muñoz, D. Errandonea, J. Ruiz-Fuertes, A. Segura, D. Santamaría-Pérez, I. M. Tiginyanu, and V. V. Ursaki, J. Appl. Phys. **111**, 013518 (2012).
[27]I. M. Tiginyanu, N. A. Modovyan, and O. D. Stoika, Fiz. Tverd. Tela (Leningrad) **34**, 967 (1992); Sov. Phys. Solid State **43**, 527 (1992).
[28]D. Errandonea, R. Boehler, S. Japel, M. Mezouar, and L. R. Benedetti, Phys. Rev. B **73**, 092106 (2006).
[29]D. Errandonea, D. Santamaria-Perez, T. Bondarenko, and O. Khyzhun, Mater. Res. Bull. **45**, 1732 (2010).
[30]D. Santamaría-Pérez, M. Marqués, R. Chuliá-Jordán, J. M. Menéndez, O. Gomis, J. Ruiz-Fuertes, J. A. Sans, D. Errandonea, and J. M. Recio, Inorg. Chem. **51**, 5289 (2012).
[31]S. Klotz, J. C. Chervin, P. Munsch, and G. Le Marchand, J. Phys. D: Appl. Phys. **42**, 075413 (2009).

[32]D. Errandonea, Y. Meng, M. Somayazulu, and D. Häusermann, Physica B **355**, 116 (2005).
[33]H. K. Mao, J. Xu, and P. M. Bell, J. Geophys. Res. **91**, 4673, doi:10.1029/JB091iB05p04673 (1986).
[34]W. Kraus and G. Nolze, J. Appl. Crystallogr. **29**, 301 (1996).
[35]G. Kresse and J. Hafner, Phys. Rev. B **47**, 558 (1993); **49**, 14251 (1994); G. Kresse and J. Furthmüller, Comput. Mater. Sci. **6**, 15 (1996); G. Kresse and J. Furthmüller, Phys. Rev. B **54**, 11169 (1996).
[36]J. P. Perdew, K. Burke, and M. Ernzerhof, Phys. Rev. Lett. **78**, 1396 (1997).
[37]J. P. Perdew, A. Ruzsinszky, G. I. Csonka, O. A. Vydrov, G. E. Scuseria, L. A. Constantin, X. Zhou, and K. Burke, Phys. Rev. Lett. **100**, 136406 (2008).
[38]N. Chetty, A. Muñoz, and R. M. Martin, Phys. Rev. B **40**, 11934 (1989).
[39]S. Baroni, S. de Gironcoli, A. Dal Corso, and P. Giannozzi, Rev. Mod. Phys. **73**, 515 (2001).
[40]Y. Le Page and P. Saxe, Phys. Rev. B **65**, 104104 (2002).
[41]O. Beckstein, J. E. Klepeis, G. L. W. Hart, and O. Pankratov, Phys. Rev. B **63**, 134112 (2001).
[42]J. F. Nye, *Physical Properties of Crystals. Their Representation by Tensor and Matrices* (Oxford University Press, 1957).
[43]H. Hahn, G. Frank, W. Klingler, A. D. Stoerger, and G. Stoerger, Z. Anorg. Allg. Chem. **279**, 241 (1955).
[44]L. Gastaldi, M. G. Simeone, and S. Viticoli, Solid State Commun. **55**, 605 (1985).
[45]E. Bandiello, D. Errandonea, D. Martinez-Garcia, D. Santamaria-Perez, and F. J. Manjon, Phys. Rev. B **85**, 024108, (2012).
[46]J. Ruiz-Fuertes, D. Errandonea, R. Lacomba-Perales, A. Segura, J. González, F. Rodríguez, F. J. Manjón, S. Ray, P. Rodríguez-Hernández, A. Muñoz, Zh. Zhu, and C. Y. Tu, Phys. Rev. B **81**, 224115 (2010).
[47]D. Santamaría-Pérez, L. Gracia, G. Garbarino, A. Beltrán, R. Chulia-Jordan, O. Gomis, D. Errandonea, Ch. Ferrer-Roca, D. Martínez-García, and A. Segura, Phys. Rev. B **84**, 054102 (2011).
[48]O. Gomis, J. A. Sans, R. Lacomba-Perales, D. Errandonea, Y. Meng, J. C. Chervin, and A. Polian, Phys. Rev. B **86**, 054121 (2012).
[49]M. D. Frogley, J. L. Sly, and D. J. Dunstan, Phys. Rev. B **58**, 12579 (1998).
[50]L. Garbato, F. Ledda, and A. Rucci, Prog. Cryst. Growth Charact. **15**, 1 (1987).
[51]C. K. Lowe-Ma and T. A. Vanderah, Acta Cryst. C **47**, 919 (1991).
[52]J. W. Earley, Am. Mineral. **35**, 337 (1950).
[53]A. Kuhn, A. Chevy, and R. Chevalier, Phys. Status Solidi A **31**, 469 (1975).
[54]S. Radescu, A. Mujica, J. López-Solano, and R. J. Needs, Phys. Rev. B **83**, 094107 (2011).
[55]U. Schwarz, D. Olguin, A. Cantarero, M. Hanfland, and K. Syassen, Phys. Status Solidi B **244**, 244 (2007).
[56]D.-W. Zhang, F.-T. Jin, and J. -M Yuan, Chin. Phys. Lett. **23**, 1876 (2006).
[57]K. Kumazaki, Phys. Status Solidi A **29**, K55 (1975).
[58]R. Hill, Proc. Phys. Soc. London, Sect. A **65**, 349 (1952).
[59]T. C. Chiang, J. Dumas, and Y. R. Shen, Solid State Commun **28**, 173 (1978).
[60]M. Gatulle, M. Fischer, and A. Chevy, Phys. Status Solidi B **119**, 327 (1983).
[61]J. M. Farley, G. A. Saunders, and D. Y. Chung, J. Phys. C: Solid State Phys. **6**, 2010 (1973).
[62]J. M. Farley and G. A. Saunders, J. Phys. C: Solid State Phys. **5**, 3021 (1972).
[63]S.-H. Ma, Z.-Y. Jiao, and X.-Z. Zhang, J. Mater. Sci. **47**, 3849 (2012).
[64]A. Reuss, Z. Angew. Math. Mech. **9**, 49 (1929).
[65]W. Voigt, *Lehrbuch der Kristallphysik* (Teubner, Leipzig, 1928).
[66]R. Caracas and T. B. Ballaran, Phys. Earth Planetary Interiors **181**, 21 (2010).
[67]Q. J. Liu, Z. T. Liu, and L. P. Feng, Commun. Theor. Phys. **56**, 779 (2011).
[68]S. F. Pugh, Philos. Mag. **45**, 823 (1954).
[69]K. Lau and A. K. McCurdy, Phys. Rev. B **58**, 8980 (1998).
[70]G. Grimvall, B. Magyari-Köpe, V. Ozoliņš, and K. A. Persson, Rev. Mod. Phys. **84**, 945 (2012).
[71]M. Born, Proc. Cambridge Philos. Soc. **36**, 160 (1940).
[72]J. Wang, S. Yip, S. R. Phillpot, and D. Wolf, Phys. Rev. Lett. **71**, 4182 (1993).
[73]J. Wang, J. Li, S. Yip, S. Phillpot, and D. Wolf, Phys. Rev. B **52**, 12627 (1995).
[74]F. Cleri, J. Wang, and S. Yip, J. Appl. Phys. **77**, 1449 (1995).